Construction and Building Materials, Vol. 170, 747-756, 2018.

GROUT-CONCRETE INTERFACE BOND PERFORMANCE: EFFECT OF INTERFACE MOISTURE ON THE TENSILE BOND STRENGTH AND GROUT MICROSTRUCTURE

De la Varga I.[1], Muñoz J.F.[1], Bentz D.P.[2], Spragg R.P.[1], Stutzman P.E.[2], Graybeal B.A[3]

[1] SES Group & Associates at Turner-Fairbank Highway Research Center, 6300 Georgetown Pike, McLean, VA, 22101 (USA).

[2] National Institute of Standards and Technology, 100 Bureau Drive, Stop 8615 Gaithersburg, MD 20899-8615 (USA).

[3] Federal Highway Administration at Turner-Fairbank Highway Research Center, 6300 Georgetown Pike, McLean, VA, 22101 (USA).

ABSTRACT

Bond between two cementitious materials is crucial in applications such as repairs, overlays, and connections of prefabricated bridge elements (PBEs), to name just a few. It is the latter that has special interest to the authors of this paper. After performing a dimensional stability study on grout-like materials commonly used as connections between PBEs, it was observed that the so-called 'non-shrink' cementitious grouts showed a considerable amount of early-age shrinkage. This might have negative effects on the integrity of the structure, due not only to the grout material's early degradation, but also to a possible loss of bond between the grout and the prefabricated concrete element. Many factors affect the bond strength between two cementitious materials (e.g., grout-concrete), the presence of moisture at the existing concrete substrate surface being one of them. In this regard, pre-moistening the concrete substrate surface prior to the application of the grout material is sometimes recommended for bond enhancement. This topic has been the focus of numerous research studies in the past; however, there is still controversy among practitioners on the real benefits that this practice might provide. This paper evaluates the tensile bond performance of two non-shrink cementitious grouts applied to the exposed aggregate surface of a concrete substrate, and how the supply of moisture at the grout-concrete interface affects the bond strength. "Pull-off" bond results show increased tensile bond strength when the concrete surface is pre-moistened. Reasons to explain the observed increased bond strength are given after a careful microstructural analysis of the grout-concrete interface. Interfaces where sufficient moisture is provided to the concrete substrate such that moisture movement from the grout is prevented show reduced porosity and increased hydration on the grout side of the interface, which is thought to directly contribute to the increased tensile bond strength.

KEYWORDS

Cementitious grout; Interface moisture; Porosity; Tensile bond strength.

BACKGROUND

The bond between cementitious materials is a topic that has been extensively researched in the past decades [1–8]. The literature has identified a number of key factors that influences the measured bond strength, including the substrate surface preparation, the use of bonding agents, the mechanical properties of the two materials, and even the test method used to assess the bond strength [1,5,9].

One parameter that is recognized to affect the bond performance between two cementitious materials is the availability of moisture at the concrete substrate surface prior to the casting of the new material [10–12]. It has been reported that when pouring a fresh material over a dry concrete substrate, the substrate may absorb part of the mixing water from the former, thus forcing the water to migrate from the new material to the substrate [13]. This effect might be more pronounced in highly fluid materials (e.g., cementitious grouts). The water migration would not only lead to internal stresses at the interface, but could also reduce the strength of the grout material due to a lack of sufficient water for its hydration. It is therefore believed that by providing extra moisture at the interface prior to the application of the fresh material, it is possible to reduce the water migration. This has been observed using neutron images [14] in repair mortar overlays cast over concrete substrates in "saturated surface dried" (SSD) conditions, compared to dry substrates.

While there is a certain degree of consensus regarding the beneficial effects of pre-moistening the substrate, there is some controversy among researchers and practitioners as to if this is really the case [11,12]. Courard, et al., have reported that there is an optimum substrate moisture range between 55 % and 90 % degrees of saturation [8]. Outside of this range of degree of saturation, the bond strength decreases. The practice of pre-moistening the concrete substrate surface in order to achieve SSD conditions has become common in the construction industry [15].

In a review of the literature of the topic, the authors have identified that recommendations to pre-moisten the substrate are dependent on the test method being used, the surface preparation techniques used, and the types of materials being bonded. This study focuses on evaluating the effect that the supply of extra moisture at a grout-concrete interface has on the bond performance, specifically targeting the potential application in connections of pre-fabricated bridge elements (PBE). For that purpose, the surface of the concrete substrate has been prepared according to current field practices (more details will be given in the next sections). This study assesses the tensile bond strength between cementitious grouts and a concrete substrate using "pull-off" bond tests. Additionally, the paper presents scanning electron microscope (SEM) images along with measured porosity and hydration profiles in the grout material along the interface with the concrete material to correlate the pull-off bond results to the grout microstructure features.

MATERIALS

Concrete

An ordinary portland cement, ASTM C150-16 Type I/II, with a Blaine fineness of 382 m^2/kg, and a density of 3070 kg/m^3, was used to prepare the concrete. The fine aggregate (FA) used was ordinary river sand with an apparent specific gravity of 2.59. The coarse aggregate (CA) consisted of dolomitic limestone with an apparent specific gravity of 2.85. The concrete mixture was developed to perform similarly to a prefabricated concrete element in terms of strength. Therefore, the concrete was designed with a water-to-cement ratio (*w/c*) of 0.35 by mass, cement:FA:CA ratio of 1:1.7:2.5 (by mass), a minimum slump of 76 mm (3 in.) (achieved by using a high-range water reducer), and a targeted 28-d compressive strength of 55 MPa (8000 psi).

'Non-Shrink' Cementitious Grouts

Two commercially-available 'non-shrink' cementitious grouts were used in the study, labelled here as Grout A and Grout B. The grouts are supplied in a bag containing the solid fraction (e.g., cementitious materials, additives, and fine aggregates) that is mixed with a certain amount of water following the manufacturer's recommendations to obtain an average flow of 100 % per ASTM C1437. Grout A requires a water-to-solids ratio (*w/s*) of 0.16 by mass and produces a 28-d compressive strength of 62 MPa (9000 psi), whereas grout B requires a *w/s* of 0.17 and provides a 28-d compressive strength of 48 MPa (7000 psi).

EXPERIMENTAL

Grout-Concrete Specimen Preparation

A concrete slab with dimensions of 914 mm x 914 mm x 102 mm (36 in. x 36 in. x 4 in.) was used as the substrate for the pull-off bond tests. The concrete slab was cured for 14 d after casting at a temperature of 23 °C ± 1 ºC (73.4 °F ± 1.8 ºF) and relative humidity of 50 % ± 5 %. (14 d was selected for convenience; the authors consider this age to be representative of the substrate age at the moment of the grout pour. 14 d curing was sufficient to provide a concrete tensile strength that was greater than that of the grout-concrete interface). The top surface of the concrete slab was pressure washed at 24 h after casting in order to create an exposed coarse aggregate interface (see Figure 1(a)), facilitated by using a commercially available in-form paint-like retarding agent. This is becoming a common substrate surface preparation method in several states for PBE connection applications [16], and it is the reason why it has been selected for this study.

A 50-mm (2-in.) thick grout overlay was cast over the top surface of the concrete slab so that an interface between the two materials is created. Moisture at the grout-concrete interface was provided by ponding the exposed aggregate concrete surface with water during the 24 h period that preceded the casting of the grout, and manually drying the surface with paper towels, so that an SSD condition was achieved. Therefore, two different types of specimens were prepared: 1) “control” (with no moisture added to the interface), and 2) “SSD” (with moisture added to the interface).

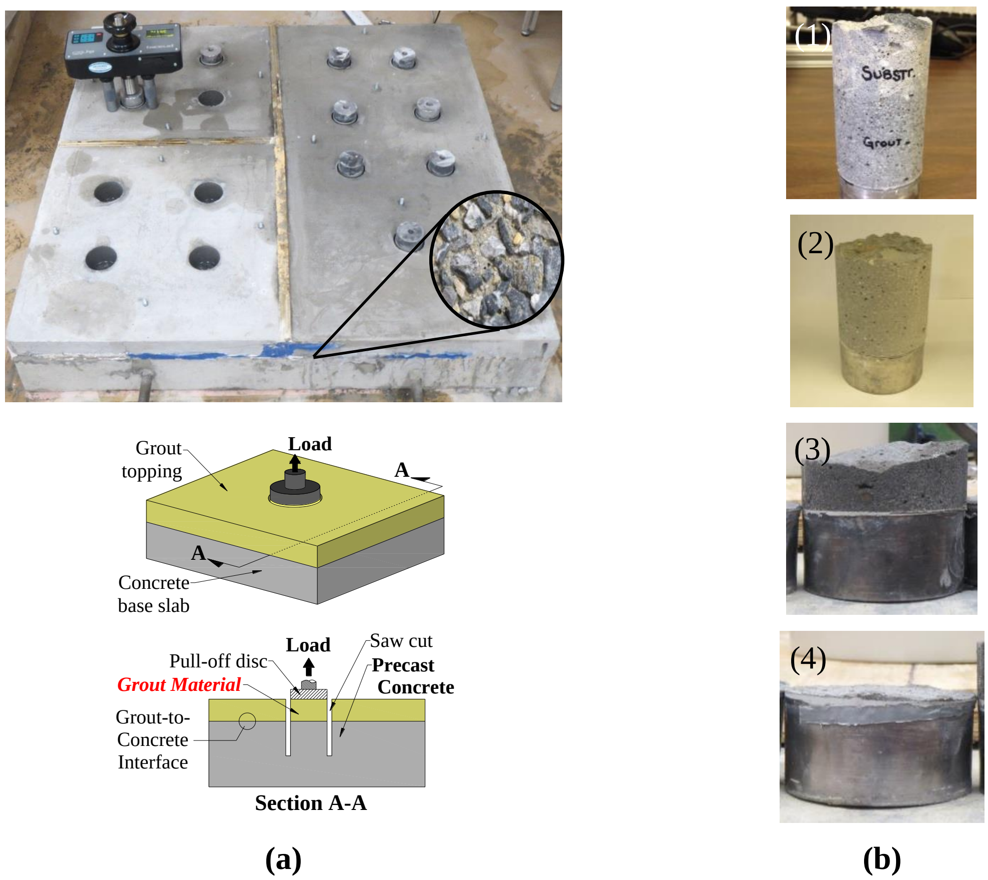

Figure 1. (a) Grout-concrete slab for pull-off tests (concrete substrate surface was prepared with an in-form retarder agent to expose the coarse aggregates, as shown in the figure) with illustration of pull-off bond test method via ASTM C1583, and (b) four possible failure modes obtained after executing pull-off tests: (1) substrate failure, (2), interface failure, (3) grout failure, (4) glue failure.

Pull-off bond tests

The bond assessment was performed according to the ASTM C1583 test method (direct tension “pull-off” test) on the grout-concrete slab (Figure 1(a)). In this test, a 50-mm (2-in) diameter steel disc is glued on the top surface of the grout. The test specimen is formed by partially drilling a core perpendicular to the surface, and penetrating down into the concrete material, approximately 25 mm (1 inch) below the grout-concrete interface. A tensile load is applied to the steel disc at a constant rate of 35 kPa/s ± 15 kPa/s (5 psi/s ± 2 psi/s) until failure occurs. The failure load and the failure mode were recorded and the nominal tensile stress could thus be calculated. If failure occurred at the grout-concrete interface, then the true bond strength could be assessed. If failure occurs in either the concrete substrate or grout material, then the tensile strength of the failing material could be assessed and the interface bond strength could be recognized to be higher than the value achieved. Finally, the test was rejected if failure occurred at the glue-grout interface (Figure 1(b)). According to the ASTM test method, at least three valid tests should be completed and the results averaged for any particular failure mode.

Microstructural analysis

After completion of the pull-off bond tests, grout-concrete specimens were prepared for microstructural analysis. Cores 50-mm (2-in.) in diameter were extracted from the grout-concrete slab and cut in half to expose the interface (Figure 2). The specimens were then immersed in isopropanol for 48 h, dried in a vacuum oven at 25 °C (77 ⁰F), impregnated with a low-viscosity epoxy resin, lapped, and polished to a surface roughness of 0.25 µm. All the cuts were performed using inorganic oil as the lubricant.

(a) (b)

Figure 2. (a) Cylindrical cores extracted from grout-concrete slab, (b) grout-concrete specimen prepared for SEM/EDS analysis.

The microstructure of the polished specimens was examined using a FEI Quanta 650[1] scanning electron microscope (SEM) equipped with a concentric backscatter detector coupled with Energy Dispersive X-ray Spectroscopy (EDS/EDX). The microscope was operated under high vacuum at 15 KV and with a 10-mm working distance. Large backscatter electron (BSE) and EDS/EDX mapping areas were collected using Aztec 2.4 EDS microanalysis software. The maps had a total of 299 fields, each one with a 3000x magnification, which covered a total area of 1.79 mm^2 (0.0028 in^2). An example of a large BSE map for a grout-exposed coarse aggregate interface is displayed in Figure 3(a). A minimum of six maps per specimen were collected in random areas,

[1] Certain commercial equipment and software are identified to describe the subject adequately. Such identification does not imply recommendation or endorsement by FHWA or NIST, nor does it imply that the equipment identified is necessarily the best available for the purpose.

covering a total area of approximately 9 mm^2 (0.014 in^2) of the interface, to ensure that the analysis was representative of each sample. The area in the large BSE maps corresponding to sand particles in the grout was removed using an image treatment process based on the EDS elemental map of calcium. Specific details of the methodology can be found in Beyene et al. [17]. The obtained map of sand particles in the grout was then subtracted from the original large BSE map to obtain the final large paste map, used for the porosity measurements, as illustrated in Figure 3(b).

The porosity of the final large paste map, as shown in Figure 3(b), was evaluated on the grout paste adjacent to the surface of the concrete, and up to 100 μm away from the latter. A porosity profile was obtained by extracting consecutive 10-μm wide bands, in a similar process to that proposed elsewhere [18,19] to characterize the interfacial transition zone around aggregates in concrete. Examples of this segmentation process and a typical 10-μm wide band are displayed in Figure 3(c) and (d), respectively.

The image analysis software ImageJ 1.49v[1] was used for quantification of the porosity in each of the BSE 10-μm wide bands. Specific details of the process to measure porosity are described in Beyene et al. [17]. It is important to mention that the pixel size in the images (1 pixel representing 0.2 µm x 0.2 µm) allowed for the quantification of pores ranging from 0.45 µm to 40 µm, herein referred to as capillary pores. The upper limit of 40 µm was selected based on the maximum pore size observed in these types of interfaces. The lower limit was selected based on the Nyquist theorem [20]. The large BSE maps displayed in this paper are representative of the entire samples. The coefficient of variation (CoV) of measured porosity on each of the 10-μm wide bands evaluated was found to be less than 8.5×10^{-4} %.

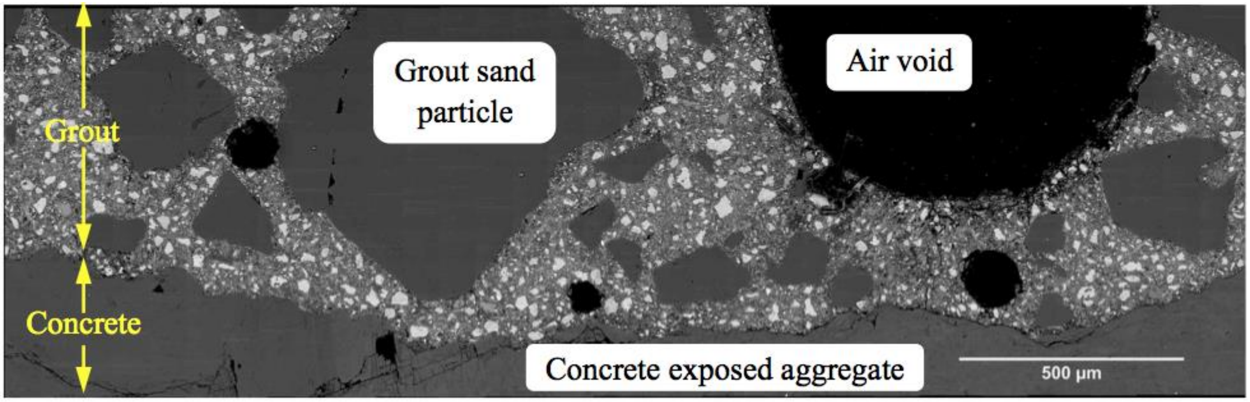

(a)

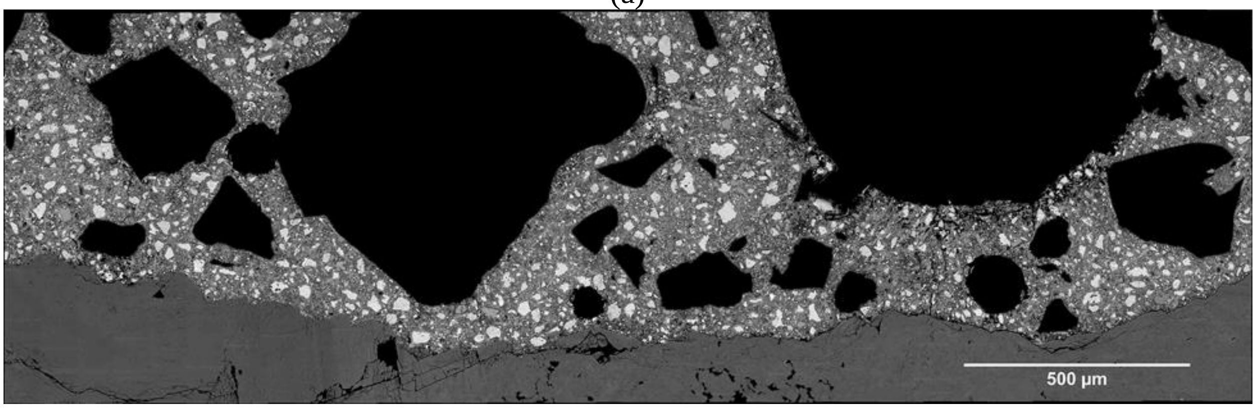

(b)

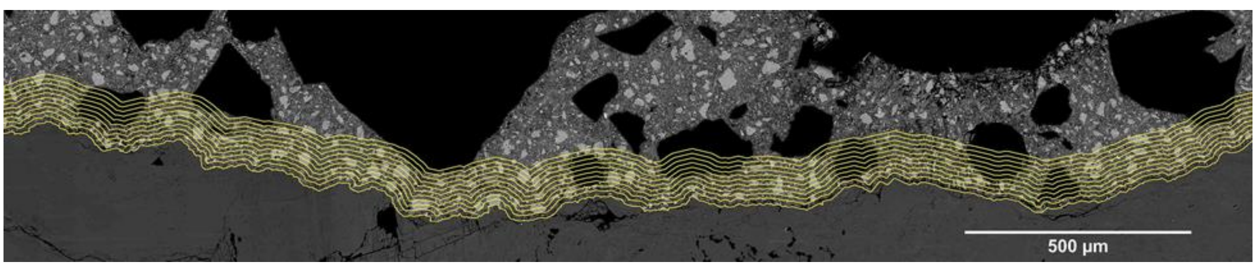

(c)

(d)

Figure 3. Example of segmentation process based on calcium EDS mapping used to study the microstructure of the grout-concrete interface. The process is illustrated with a large map of a control sample cured for a total of 14 d on the specific grout-exposed aggregate region: (a) original large BSE map, (b) large paste map after removal of grout sand particles, (c) location along the interface of the 10-μm wide bands, and (d) example of a 10-μm wide band extracted 20 μm away from the exposed aggregate surface.

RESULTS

Pull-off bond tests

Table 1 shows the pull-off bond strength results obtained for various batches of the two cementitious grouts used in the study and applied to an exposed aggregate concrete substrate surface. The results were collected over a period of about two years, and the variability in the results observed within Grout A are attributed to potential modifications in the product formulation made by the manufacturer during this time. Results labelled as “control” correspond to the specimens where no moisture was added (i.e., specimens were maintained at drying conditions in a room that holds the temperature and relative humidity at 23 °C ± 1 ºC (73.4 °F ± 1.8 ºF) and 50 % ± 5 %, respectively). “SSD” corresponds to the specimens where additional moisture was provided via 24-h water ponding and subsequent paper towel drying. All the specimens failed at the grout-concrete interface, so the (theoretically) true bond strength was assessed. In all cases, the bond strength increased when an SSD condition was provided on the concrete surface, doubling the bond strength with respect to the control in some cases (percentage increase is shown in the table). In five out of the nine cases presented, the bond strength mean values for the two surface conditions (SSD and control) were statistically different at the 0.05 significance level.

Table 1. Results of direct tension (pull-off) testing (Control vs. SSD) for various batches of two cementitious grouts throughout the period of 2 years.

Material	Batch	Grout Age at Test (d)	Control (MPa)	SSD (MPa)	Control (psi)	SSD (psi)	Bond Strength Increase (%)	$t_{0.05}$
Grout A	1	2	1.90 ± 0.40	2.68 ± 0.44	276 ± 57	389 ± 64	41	N
		14	2.77 ± 0.25	3.46 ± 0.50	402 ± 37	501 ± 72	25	Y
	2	14	2.37 ± 0.16	2.73 ± 0.61	343 ± 23	397 ± 88	16	N
	3	14	2.67 ± 0.55	2.81 ± 0.14	387 ± 80	408 ± 21	5	N
	4	7	1.79 ± 0.67	3.70 ± 0.26	259 ± 98	536 ± 38	107	Y
	5	14	3.78 ± 0.36	4.50 ± 0.23	549 ± 52	652 ± 34	19	N
	6	14	1.49 ± 0.23	3.04 ± 0.56	216 ± 34	441 ± 82	104	Y
Grout B	1	2	1.82 ± 0.12	2.74 ± 0.42	263 ± 18	398 ± 62	51	Y
		14	2.06 ± 0.57	3.18 ± 0.36	300 ± 82	461 ± 52	54	Y

Microstructural analysis

The microstructural analysis of the grout-concrete interface (hereafter referred to as just “interface”) was performed only on some grout-concrete specimens collected from the pull-off tests using grout A (see highlighted cases in Table 1). This material was chosen over grout B, since the latter contained a specific component in its original formulation that triggered a gas reaction during the curing process. Evidences of this gas reaction in grout B were observed by the presence of uniformly distributed air bubbles ranging from 50 µm to 150 µm during a preliminary SEM analysis of fresh fracture surfaces of the interface. (Some cementitious grouts are designed to counteract later age hydration-related shrinkage by adding expansive agents, including some that generate gases). As such, in order to eliminate the gas formation as an additional variable that might have an effect of the final interface microstructure, only grout A was selected for further microstructural investigation.

The microstructural analysis presented in this paper corresponds only to the grout side of the interface. It is therefore assumed that the microstructural characteristics of the substrate in both "control" and "SSD" conditions would be very similar. This was in fact confirmed by an SEM porosity analysis of thin sections prepared from concrete specimens extracted prior to the grout pour. Despite submerging the concrete surface during 24 h to achieve the SSD moisture condition (which might further hydrate the paste at the concrete surface), no significant differences in the measured porosity were observed between the control and SSD concrete specimens. The porosity values in both the control and SSD concrete ranged from 0.60 % to 0.65 % in the areas close to the concrete surface (from 0 µm to 20 µm of distance) down to 0.20 % in those areas farther away (from 90 µm to 100 µm). The percent porosities were within 0.05 of one another for the two conditions.

Interfaces are commonly seen as lines (in 2D images) or planes (in 3D images) between two different phases (e.g., materials). This is easy to observe when the two phases (or materials) are different in terms of, for instance, porosity (e.g., aggregate-paste interface). However, this approach proves to be difficult for interfaces formed between cementitious materials, especially in paste-to-paste interfaces, where both materials show similar microstructures in terms of porosity. As such, in this paper an interface was considered more as a region (that is, a plane in 2D images, or a volume in 3D images), including areas that extend several microns within the two interfacial materials. It is also worth mentioning that heterogeneity is one of the principal attributes of an interface at a micro-scale level. This further complicated the possibility of obtaining representative porosity measurements even though large maps were used in the evaluation. Even so, two different areas could be distinguished at the interface since the grout was poured over a concrete surface where the coarse aggregate was previously exposed. The first area corresponded to that where the grout is in direct contact with the exposed coarse aggregate of the concrete material (G-A interface), while the second area represented locations where the grout is in direct contact with the paste fraction of the concrete material (G-P interface). This latter area is typically confined between exposed coarse aggregate particles, creating a "valley-like" configuration with the paste at the bottom. An illustration of G-A and G-P interfaces is shown in Figure 4. As already mentioned only the grout side of the interface was analyzed in this paper.

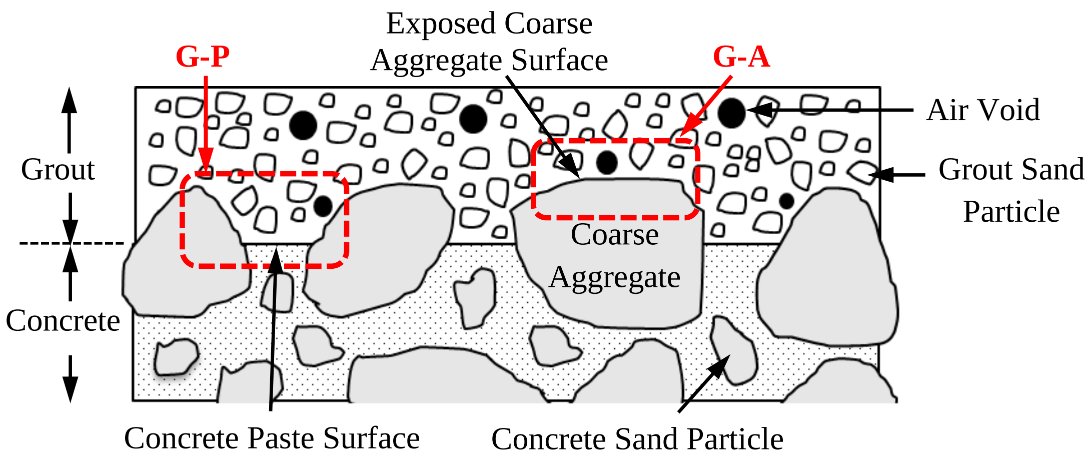

Figure 4. Illustration of G-A and G-P interfaces in a grout-concrete interface with exposed coarse aggregate on the concrete side. Note: the illustration is not to scale.

Examples of representative large maps of G-A interfaces are displayed in Figures 3(a) and 5. As observed, the resulting microstructure of a G-A interface is characterized by an "unconfined" configuration, which makes it easy for the grout to consolidate. The "unconfined" microstructure contributed to minimize the commonly-known "wall effect" [18,21–23], which would reduce the packing efficiency of the grout particles at the vicinity of the exposed coarse aggregate surface. The consequence of this "unconfined" structure was a dense microstructure at the interface with a reduced porosity in the grout. However, local disturbances in the packing efficiency that created "pockets" of porosity were common in this type of interface. These porosity "pockets" were caused by the proximity of sand particles and/or air voids to the exposed coarse aggregate surfaces, as well as the confluence of several sand particles at the interface region. Examples of these localized disturbances in the packing efficiency are depicted in Figure 5 as Area A (for sand particles) and Area B (for air voids). It is important to mention that "porosity pockets" caused by the proximity of sand particles can also be found in bulk areas of the sample, a few hundreds of microns away from the exposed coarse aggregate surface (Area C in Figure 5). However, the influence of these high porosity areas in the bulk was disregarded in the porosity evaluation presented in this paper by limiting the area of interest to being within 100 μm of the exposed coarse aggregate surfaces (G-A interfaces) or concrete paste surfaces (G-P interfaces).

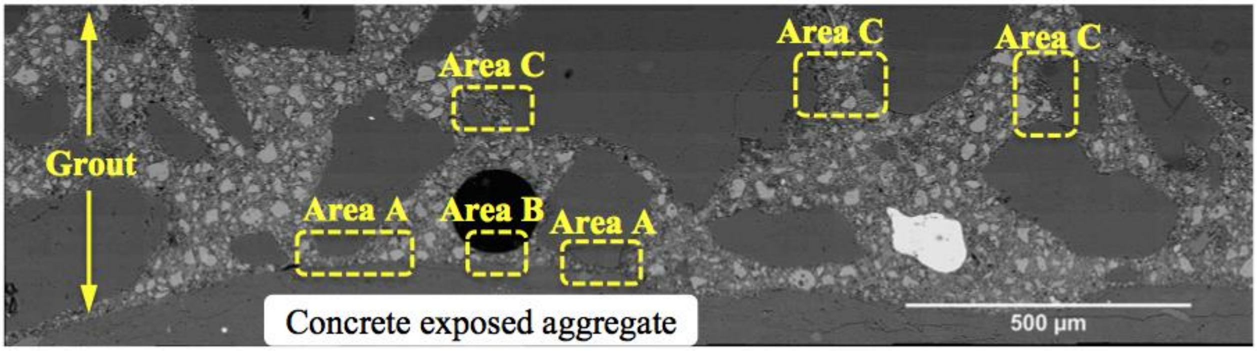

Figure 5. Large BSE map of a G-A interface of a control (non-SSD) sample cured for 2 d. It shows an "unconfined" configuration that facilitated the packing of the grout particles on top of the exposed coarse aggregate surface. Local porosity was created at the interface by the presence of sand particles of the grout (Area A) or air voids (Area B). The same phenomenon was observed in the bulk (Area C).

When quantifying the amount of porosity in G-A interfaces, it is observed that the presence of sand particles has an influence on the total porosity. This is illustrated in Figure 6, where sudden increases in the porosity fraction (indicated by dashed arrows) occurred as we approach the exposed coarse aggregate surface in locations where sand particles were present. In other words, porosity tended to increase in between the sand and exposed coarse aggregate particles, especially near sand particles. This effect was observed regardless of the curing time (2 d or 14 d) and the type of sample (control or SSD). Therefore, SSD conditions did not have any effect on the microstructure of G-A interfaces, at least in terms of the measured porosity.

Contrary to G-A interfaces, the microstructure of G-P interfaces was highly influenced by a "confined" configuration, due mainly to the proximity of exposed coarse aggregates from the concrete material (previously expressed as "valley"-like regions). The configuration caused a poor packing efficiency of the grout in these regions, as reflected by the large porosity observed in Figure 7. The presence of large sand particles in such a confined environment actively contributed to further increase the porosity. This resulted in the presence of pores with sizes up to 40 μm.

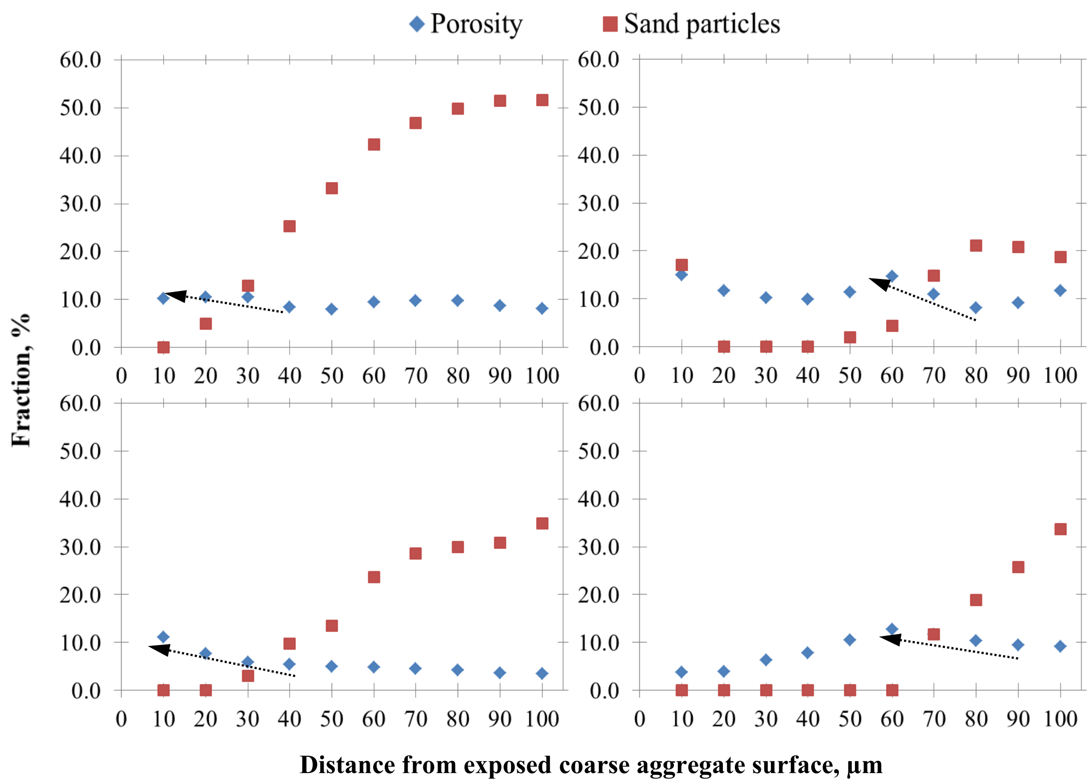

Figure 6. Influence of the presence of sand particles on the total porosity at four G-A interfaces (Based upon a single measurement).

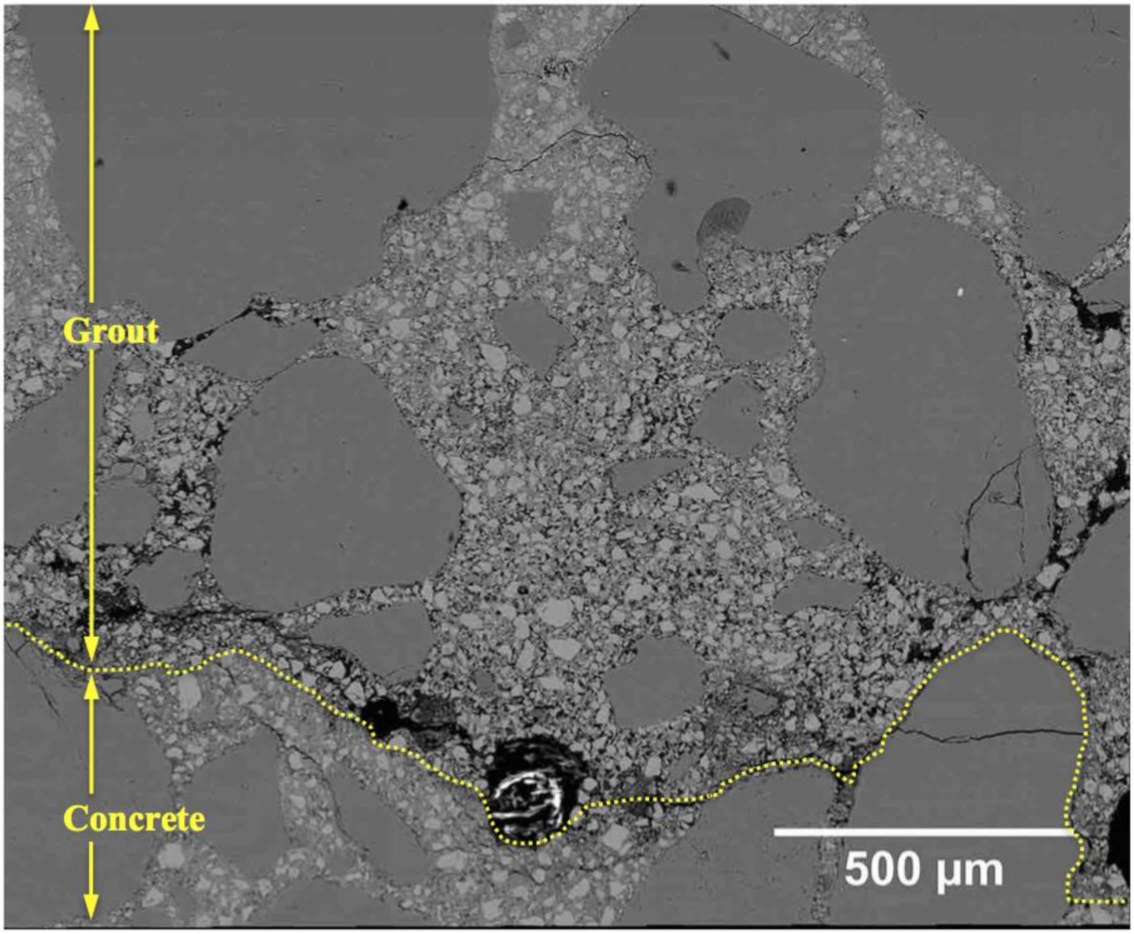

Figure 7. Large BSE map of a G-P interface of a control (non-SSD) sample cured for 2 d. It shows a "confined" configuration that impaired proper packing of the grout.

Quantification of the overall porosity distribution of the grout as a function of distance from the concrete surface (either exposed aggregate or paste surfaces) is presented in Figure 8. The results include both types of interfaces (G-A and G-P) for the two types of tested specimens (control and SSD) and cured for 2 d and 14 d. Several general observations can be made from the results. First, all the tested samples showed significant porosity values within the analyzed 100 μm band. The values ranged from about 10 % to 30% in the areas close to the concrete surface (from 0 μm to 20 μm of distance), down to approximately 5 % in those areas farther away (about 90 μm to 100 μm). The values of porosity progressively decreased in moving away from the concrete surface. This tendency was occasionally disrupted, causing a peak in porosity, due to the proximity of sand particles (as previously explained in the paper). These peaks in porosity were mostly a characteristic of the G-A interfaces as shown in Figure 8 for the SSD specimen at 14 d.

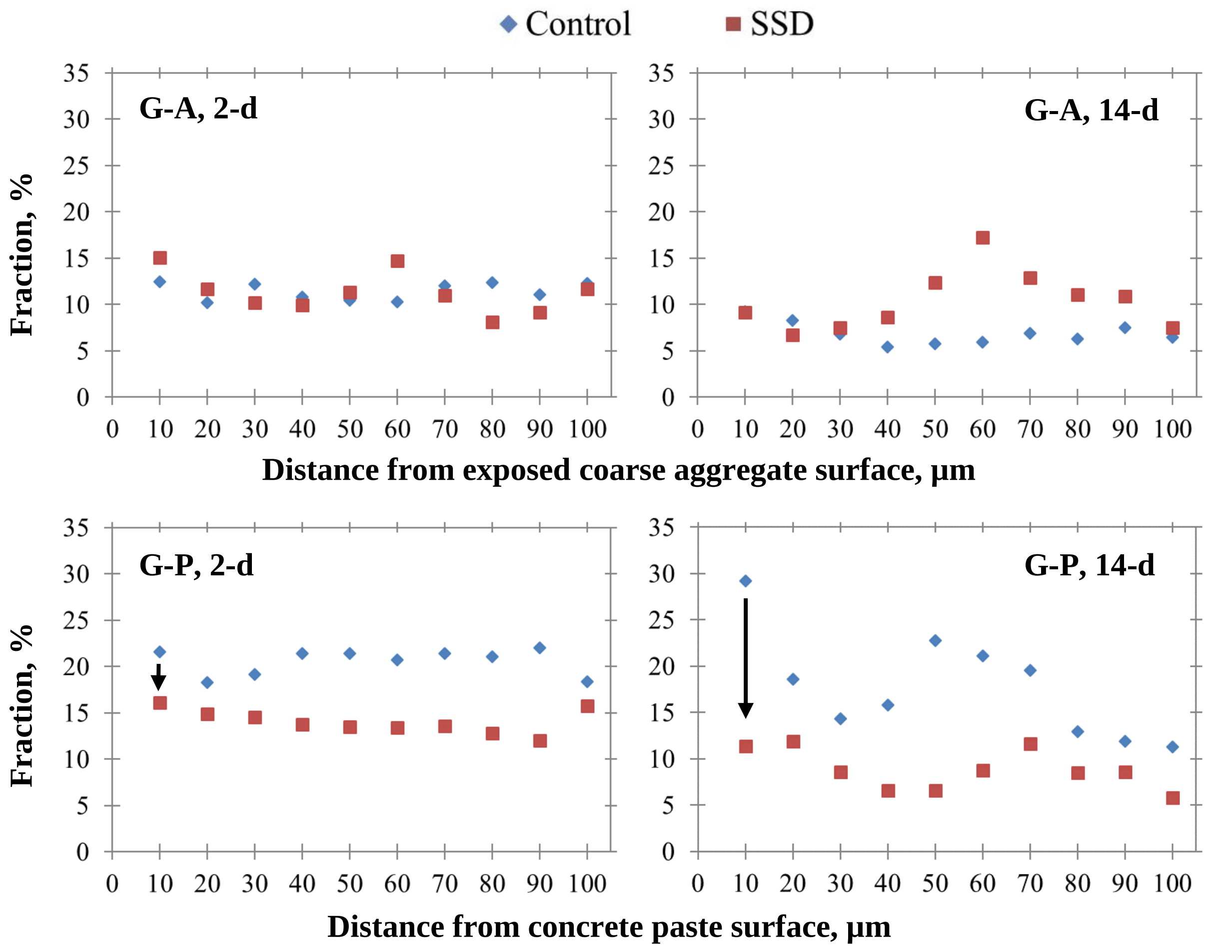

Figure 8. Overall porosity distribution of the grout (including both G-A and G-P interfaces). (These plots are based on averaged measurements of three representative areas. While the CoV was below 15 % in the 0 to 20 µm bands, this value is less homogeneous in the rest of the bands, achieving values of 50 %. This high variability is caused by the presence of sand particles near the interface, as shown in figure 6).

When comparing the porosity distribution in the two types of interfaces studied (G-A vs. G-P), it can be observed that for G-A interfaces, the maximum porosity within the first 20 µm was approximately between 10 % and 15 %. This number slightly decreased to 5 % to 10 % by the end of the 100 µm band. The increase of grout curing time from 2 d to 14 d did not cause a significant reduction in the measured porosity (between 0.2 µm to 40 µm pore size) regardless of the type of specimen, control or SSD. On the other hand, porosity values in G-P interfaces were not significantly affected by the increase in curing time; however, the values were influenced by the type of specimens. In general, porosity in the first 20 µm band of G-P interfaces was higher for the control (around 22 % and 30 % at 2 d and 14 d, respectively) than for SSD specimens (18 % and 13 % at 2 d and 14 d, respectively). The reduction in porosity in the SSD specimen with respect to the control is indicated by the arrows in Figure 8. A closer comparison of the pore size distribution of each band within the first 40 µm for the 14-d G-P interfaces in the control and SSD specimens provides additional information, as illustrated in Figure 9. The higher overall porosity in the control with respect to the SSD specimen was caused by a higher number of larger capillary pores (25 µm to 40 µm in size) at 10 µm and 20 µm distances from the concrete paste surface. At larger distances from the surface, both specimens had similar porosity size distributions.

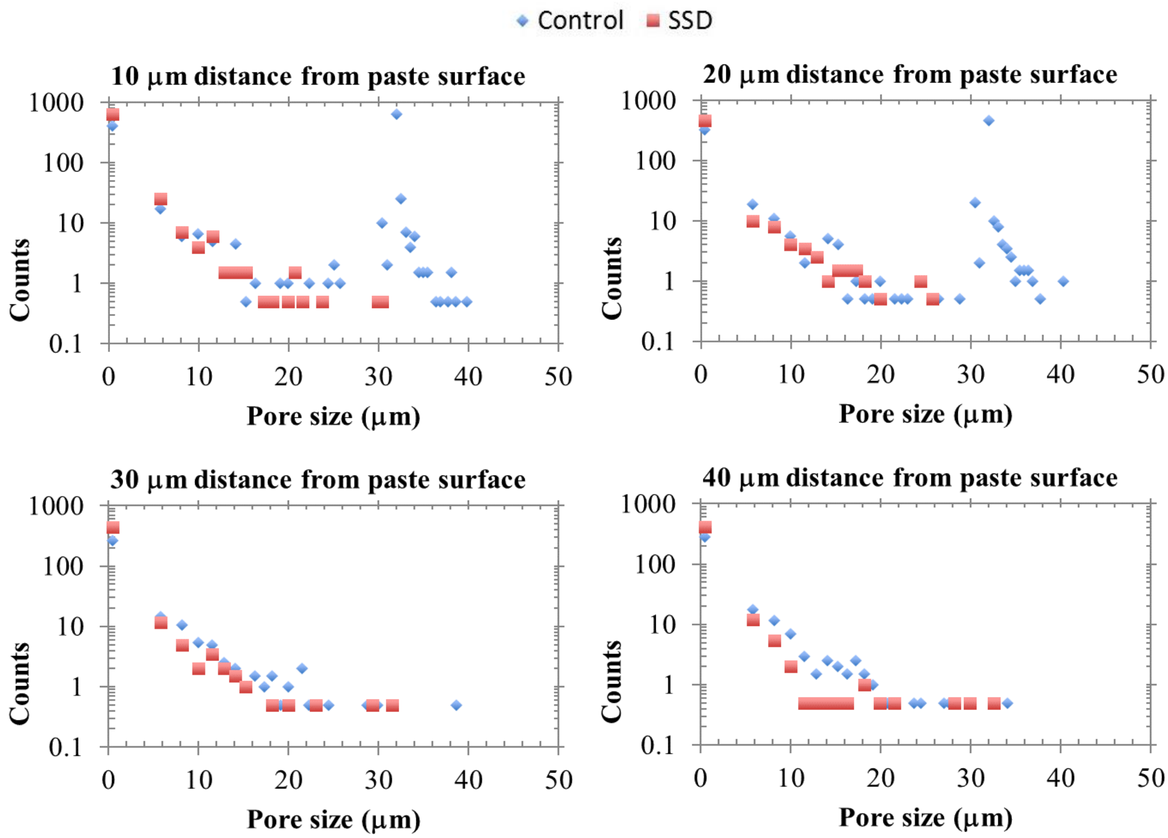

Figure 9. Comparison of pore size distribution analysis in 14-day G-P interfaces between the control and SSD specimens

The difference in overall porosity and pore size distribution in the first 20 µm at G-P interfaces can be attributed to one of the two following mechanisms. The first mechanism assumes that the presence of water in the capillary pores of the concrete paste in the SSD sample did help in reducing the higher porosity and refining the pore size distribution by maximizing the formation of hydration products at the grout side of the interface. Theoretically, neither unhydrated solids nor porosity will contribute much to bonding. For this reason, the amount of hydration products was measured on G-P interfaces in the 14 d specimens (both Control and SSD). Figure 10 shows that the amount of hydration products in the SSD specimen is significantly higher at the 0.05 significance level than that of the control specimen throughout the entire 100 µm band that was analyzed, and particularly in the 10 µm band adjacent to the existing substrate. The differences in hydrated and unhydrated volume fractions between the control and SSD conditions are much greater than their difference in porosity (Figure 8).

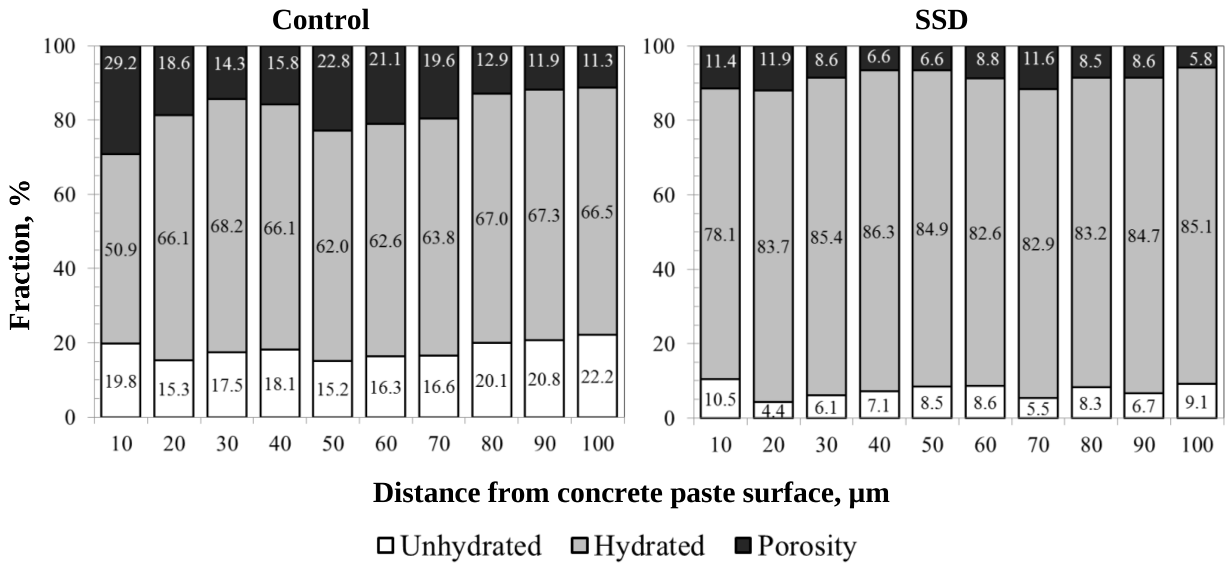

Figure 10. Overall porosity, hydrated, and unhydrated distribution on the grout side of the interface in 14 d G-P interfaces, for both control and SSD specimens. (These plots are based on averaged measurements of three representative areas. The CoV was below 15 %).

The second mechanism would consist of a moisture-air exchange occurring between the grout and concrete materials. In other words, the air present in the concrete's capillary pores would migrate into the grout as the moisture in the grout is absorbed by the concrete substrate. This has been observed by other researchers [13]. According to this mechanism, the migrated air should remain as (circular) voids near the interface. The extent of this mechanism was determined by analyzing the degree of circularity of the previously identified porosity in the first 40 µm at G-P interfaces. It was assumed that circularity values of air voids will be close to one; while circularity values close to zero will be indicative of voids caused by packing deficiencies. The results in the circularity index for both samples are shown in Figure 11. The overall low circularity values of the porosity, close to 0, support that a poor consolidation of the grout onto the exposed concrete aggregate surface was the main cause of the higher and coarser porosity in the control specimens in this case.

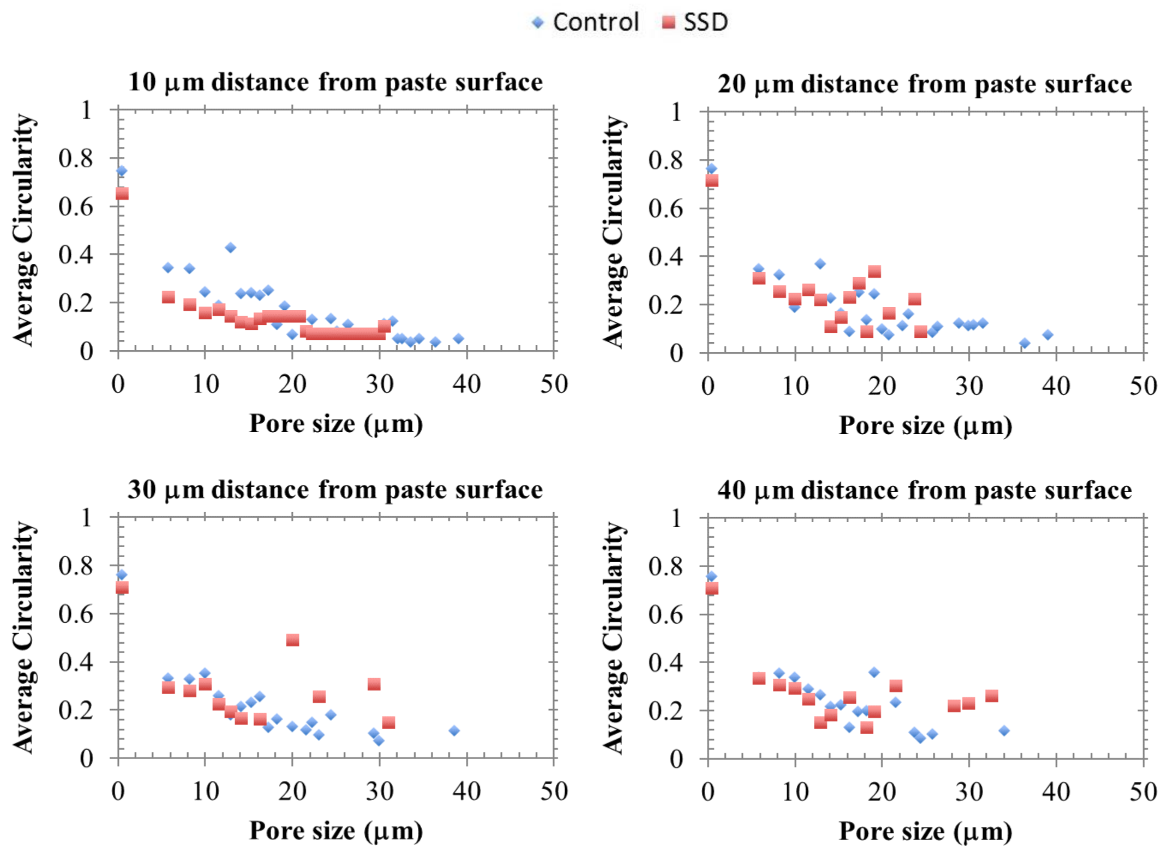

Figure 11. Circularity index analysis of the porosity for the 14-day G-P interfaces of the control and SSD specimens.

DISCUSSION

The pull-off bond results obtained in this study show a clear effect of pre-moistening the concrete surface prior to the grout pour by using the SSD approach explained above. The tensile bond strength is increased by up to 107 % in some cases. These are significant increases that merit a closer look. As such, SEM images and porosity profiles of the grout along the interface have been used to better understand the mechanism behind the enhanced bond performance.

In the case presented here, the concrete surface has been treated with a retarder so that the coarse aggregate fraction is exposed. This implies that the grout-concrete contact occurred in two different types of surfaces: exposed coarse *aggregate* and concrete *paste* surfaces, respectively creating two types of interfaces named here as G-A and G-P. While G-A interfaces were characterized by a more "unconfined" microstructure, G-P interfaces tended to be more "confined", typically in between exposed coarse aggregate particles, forming "valley-like" regions. G-A interfaces occupied about 70 % of the entire concrete surface based on the mixture design used in this study, and typically provide initial bond strength through mechanical interlock, as shown elsewhere [24].

Most of the SEM images collected showed grout packing deficiencies and increased local porosity for the particular grout used in the study (grout A) in both G-A and G-P interface types (the authors mainly attribute this to non-optimum gradation of sand and fillers in the grout formulation). Even so, the grout tended to consolidate much better over G-A interfaces than over G-P interfaces, due mainly to the more "unconfined" configuration of G-A interfaces as opposed to that of G-P interfaces (more "confined"). This resulted in a poor grout consolidation in G-P interfaces, thus depicting a more porous type of microstructure. In addition to this, water migration is more common at these G-P interfaces since water is moving from one porous material (grout) into another porous material (concrete paste). The consequence of this is that the grout may not properly hydrate in the control sample (non-SSD) due to a lack of available water needed for hydration. Therefore, it is expected that SSD conditions will be beneficial in this regard, especially in G-P interfaces.

When evaluating the effect that SSD conditions had on the amount of porosity found in each of these interface types, it was found to have a different effect. In G-A interfaces, similar porosity values (approximately 0.50 %) were found at the vicinity of the concrete surface regardless of the moisture condition (control or SSD). This makes sense as it is not expected that a film of free water stays over the exposed coarse aggregate surface when applying the SSD condition (as surfaces were manually-dried with paper towels). Therefore, it can be inferred that SSD conditions did not really change the moisture conditions in G-A interfaces. On the other hand, G-P interfaces showed clear differences in the measured porosity near the concrete paste surface (especially within the first 20 μm), with reduced values in the SSD samples (approximately 15 %, compared to 30 % in control samples at 14 d). As already mentioned, water migration is more common at these G-P interfaces. For the control samples, as water is absorbed by the substrate, the cement particles in the grout will be drawn into a more tightly packed (denser) configuration at the interface, as supported by the plots in Figure 10. Water removal from the grout at this interface will also increase its viscosity (and yield stress), so that the grout will not easily conform to the rough concrete surface and "pockets" of porosity (non-circular pores) will remain. Conversely, it is believed that SSD helps in preventing (or at least reducing) this water (and particle) movement by keeping the capillary pores of the concrete substrate "more saturated", while at the same time increasing the degree of hydration of the grout (denoted by the reduced measured porosity and increased hydration products), as shown in figure 10. The increased degree of hydration observed in SSD samples compared to the control would imply not only improved mechanical properties of the grout (e.g., tensile strength), but also more hydration products in direct contact with the concrete surface. These two aspects (better mechanical properties and higher degree of hydration) may explain the increased bond strength observed in the SSD samples.

More hydration products forming in SSD samples would also mean that larger contact areas exist between the grout and the concrete at the interface. This raises questions such as the type of crystals forming when SSD conditions are provided, compared to those in the control. It is believed that SSD conditions would not only increase the degree of hydration in G-P interfaces, but would also concurrently cause the formation of thicker (and probably stronger) crystal structures that would provide larger contact areas with the concrete surface. This topic is being further investigated. Additionally, less porous G-P interfaces should mean more durable bonds, an important aspect when evaluating the long-term performance of the grout-concrete interface that requires more research.

It has then been shown that SSD conditions have a major contribution in reducing the measured porosity and increasing the volume fraction of hydration products in G-P interfaces for the materials examined in this study, thus increasing the tensile bond strength. This is especially evident in the type of exposed aggregate concrete substrate surface presented in this paper. During the preparation of this paper, other pull-off bond results were collected on sandblasted concrete surfaces, and different effects were observed (that is, SSD was not as beneficial as in an exposed coarse aggregate surface). It is then conjectured that providing interface moisture is beneficial in interfaces where "valley-like" regions are present, as the moisture can improve the consolidation, hydration and porosity properties of those regions. All this indicates that not only the bond test method used but also the type of substrate surface preparation play an important role in the effect that interface moisture has on the bond performance. As such, it is important to note that the conclusions made in this paper only apply to this type of grout-concrete interface and for tensile pull-off testing, which was specifically chosen to target connections in precast bridge elements.

CONCLUSIONS

This paper focuses on evaluating the tensile bond performance of cementitious grouts to an exposed aggregate concrete substrate surface by means of pull-off tests and consequent microstructural (i.e., porosity) characterization of the grout-concrete interface. Based on the results obtained, the following conclusions can be made:

- For the case of coarse aggregate exposure, the presence of moisture on the concrete surface supplied in this case as SSD conditions prior to the grout placement has been demonstrated to have benefits in terms of enhanced tensile bond strength, achieving in some cases up to a 107 % increase compared to a control (dry) specimen. This contradicts some other research studies, such as the one presented by Beushausen et al. [12], where other bond test methods and/or substrate surface preparation were employed..
- The use of a retarder to provide an exposed coarse aggregate type of surface on the concrete substrate leads to the formation of two types of interfaces: 1) grout-aggregate (G-A), and 2) grout-paste (G-P). The consolidation of the grout is favored on G-A interfaces, characterized by a more "unconfined" configuration, compared to that of G-P interfaces, shown to have a more "confined" configuration. The main consequence of this is higher porosity values

observed in G-P interfaces as compared to G-A interfaces, particularly under dry surface conditions.

- The presence of moisture in the SSD specimens actively contributed to the reduction of the initial larger porosity observed in G-P interfaces, increasing the degree of hydration and the volume fraction of formed hydration products. It is then conjectured that this “densification/enhanced hydration” of G-P interfaces, together with the (very likely) stress reduction caused by the reduction of water migration shown elsewhere [14], is the main cause of the increased tensile bond strength observed in the pull-off tests.
- It has been shown that more hydration products are formed in G-P interfaces, directly contributing to the densification of the grout-concrete interface, and thus increasing the tensile bond strength.

Finally, the authors recommend pre-moistening the concrete substrate surface to enhance the tensile bond performance of a grout-exposed aggregate concrete element. This type of interface is common in PBE connection applications. Bond improvement might not be considerable, but is often significant. The provision of moisture at the interface could be a feasible means to improve tensile bond, among other available techniques (e.g., surface preparation, bonding agents, etc.).

ACKNOWLEDGEMENTS

The authors would like to thank Daniel Balcha and Michael Gregory of SES Group & Associates for their technical assistance. The research which is the subject of this document was funded by the U.S. Federal Highway Administration. This support is gratefully acknowledged. The publication of this report does not necessarily indicate approval or endorsement of the findings, opinions, conclusions, or recommendations either inferred or specifically expressed herein by the Federal Highway Administration, the National Institute of Standards and Technology, or the United States Government. The reviews of Dr. Scott Jones, Dr. Chiara Ferraris, and Dr. Ken Snyder (NIST) and Dr. Jussara Tanesi (SES Group) are greatly appreciated.

REFERENCES

[1] A. Momayez, M.R. Ehsani, A.A. Ramezanianpour, H. Rajaie, Comparison of methods for evaluating bond strength between concrete substrate and repair materials, Cem. Concr. Res. 35 (2005) 748–757. doi:10.1016/j.cemconres.2004.05.027.

[2] J. Silfwerbrand, Shear bond strength in repaired concrete structures, Mater. Struct. 36 (2003) 419–424. doi:10.1007/bf02481068.

[3] J. Silfwerbrand, Improving bonding in repaired bridge decks, Concr. Int. (1990) 61–66.

[4] J. Silfwerbrand, Bonded concrete overlays - Research eeds, in: 2nd Int. Symp. Adv. Concr. through Sci. Eng., Qubec City (Canada), 2016: pp. 193–205.

[5] J. Silfwerbrand, H. Beuhausen, Bonded concrete overlays–bond strength issues, in: Int. Conf. Concr. Repair, Rehabil. Retrofit., Cape Town, 2005: pp. 19–21.

[6] J. Silfwerbrand, J. Paulsson, Better Bonding of Bridge Deck Overlays, Concr. Int. October (1998) 56–61.

[7] B.A. Tayeh, B.H. Abu Bakar, M.A. Megat Johari, Characterization of the interfacial bond between old concrete substrate and ultra high performance fiber concrete repair composite, Mater. Struct. 46 (2012) 743–753. doi:10.1617/s11527-012-9931-1.

[8] L. Courard, J.F. Lenaers, F. Michel, A. Garbacz, Saturation level of the superficial zone of concrete and adhesion of repair systems, Constr. Build. Mater. 25 (2011) 2488–2494. doi:10.1016/j.conbuildmat.2010.11.076.

[9] J.S. Wall, N.G. Shrive, Factors Affecting Bond Between New and Old Concrete, Mater. J. 85 (1988) 117–125.

[10] A.J. Shearrer, K.A. Riding, R.J. Peterman, Effects of Concrete Moisture on Polymer Overlay Bond Over New Concrete, K-TRAN: KSU-13-3. (2015).

[11] H. Beushausen, The Influence of Precast Surface Moisture Condition on Overlay Bond Strength, Concr. Plant Int. 1 (2015) 144–147.

[12] H. Beushausen, B. Höhlig, M. Talotti, The influence of substrate moisture preparation on bond strength of concrete overlays and the microstructure of the OTZ, Cem. Concr. Res. 92 (2017) 84–91. doi:10.1016/j.cemconres.2016.11.017.

[13] M. Lukovic, G. Ye, Effect of moisture exchange on interface formation in the repair system studied by X-ray absorption, Materials (Basel). 9 (2016). doi:10.3390/ma9010002.

[14] D.P. Bentz, 30 Years of Imaging and Modeling Building Materials at NBS/NIST: From PIXAR to MICROCHAR, in: Imaging Constr. Mater. Geomaterials, Paris, France, 2016.

[15] B. Bissonnette, A. Vaysburd, K. Von Fay, Best Practices for Preparing Concrete Surfaces Prior to Repairs and Overlays, Denver, CO, 2012.

[16] Z. Haber, I. De la Varga, B.A. Graybeal, Performance of grouted Connections for prefabricated Bridge Elements. Part II: Component-Level Investigation on bond and Cracking, in: 2016 PCI Conv. Natl. Bridg. Conf., Nashville, TN, 2016.

[17] M. Beyene, J.F. Munoz, R. Meininger, C. Di Bella, Effect of Internal Curing as Mitigation to Minimize ASR Damage, ACI Mater. J. (n.d.) (submitted).

[18] S. Diamond, J. Huang, The ITZ in concrete - a diff€ erent view based on image analysis and SEM observations, Cem. Concr. Compos. 23 (2001) 179–188.

[19] A. Elsharief, M.D. Cohen, J. Olek, Influence of aggregate size, water cement ratio and age on the microstructure of the interfacial transition zone, Cem. Concr. Res. 33 (2003) 1837–1849. doi:10.1016/S0008-8846(03)00205-9.

[20] J.B. Pawley, Fundamental Limits in Confocal Microscopy, in: Handb. Biol. Confocal Microsc., Springer US, Boston, MA, 2006: pp. 20–42. doi:10.1007/978-0-387-45524-2_2.

[21] J.P. Ollivier, J.C. Maso, B. Bourdette, Interfacial transition zone in concrete, Adv. Cem. Based Mater. 2 (1995) 30–38. doi:10.1016/1065-7355(95)90037-3.

[22] K.L. Scrivener, A.K. Crumbie, P. Laugesen, The Interfacial Transition Zone (ITZ) Between Cement Paste and Aggregate in Concrete, Interface Sci. 12 (2004) 411–421. doi:10.1023/B:INTS.0000042339.92990.4c.

[23] E.J. Garboczi, D.P. Bentz, Digital simulation of the aggregate–cement paste interfacial zone in concrete, J. Mater. Res. 6 (1991) 196–201. doi:10.1557/JMR.1991.0196.

[24] I. De la Varga, Z. Haber, B.A. Graybeal, Bond of Field-Cast Grouts to Precast Concrete Elements. FHWA-HRT-16-081, McLean, VA, 2017.